Water Science and Engineering, 2009, 2(4): 16-27
doi:10.3882/j.issn.1674-2370.2009.04.002

http://kkb.hhu.edu.cn
e-mail: wse@hhu.edu.cn

Comparison and analysis of bare soil evaporation models combined with ASTER data in Heihe River Basin

Yan-xia KANG*, Gui-hua LU, Zhi-yong WU, Hai HE

Research Institute of Water Problems, Hohai University, Nanjing 210098, P. R. China

Abstract: Based on ASTER (Advanced Spaceborne Thermal Emission and Reflection Radiometer) remote sensing data, bare soil evaporation was estimated with the Penman-Monteith model, the Priestley-Taylor model, and the aerodynamics model. Evaporation estimated by each of the three models was compared with actual evaporation, and error sources of the three models were analyzed. The mean absolute relative error was 9% for the Penman-Monteith model, 14% for the Priestley-Taylor model, and 32% for the aerodynamics model; the Penman-Monteith model was the best of these three models for estimating bare soil evaporation. The error source of the Penman-Monteith model is the neglect of the advection estimation. The error source of the Priestley-Taylor model is the simplification of the component of aerodynamics as 0.72 times the net radiation. The error source of the aerodynamics model is the difference of vapor pressure and neglect of the radiometric component. The spatial distribution of bare soil evaporation is evident, and its main factors are soil water content and elevation.

Key words: *ASTER; bare soil evaporation; Penman-Monteith model; Priestley-Taylor model; aerodynamics model*

1 Introduction

The quantity of soil evaporation is significant in land-surface physical processes at regional and global scales, especially in relation to mass and energy exchange between the earth and the atmosphere. In semiarid or arid regions, soil evaporation makes up a great proportion of this exchange, not only from bare soil areas, but also from cropland. Quantification of bare soil evaporation helps us understand patterns of climate change and reduce the depletion of water in bare soil. However, two problems need to be solved.

The first problem is how to determine bare soil evaporation, which is difficult to measure directly. Many authors have recommended different models to simulate bare soil evaporation in order to solve this problem. Desborough et al. (1996) used the aerodynamics model, the Penman-Monteith model, and the Priestley-Taylor model to simulate bare soil evaporation, and the results showed that the bare soil evaporation calculated by different models varies over a wide range. It is necessary to evaluate the inconsistencies. Alvenäs and Jansson (1997)

This work was supported by the Ministry of Water Resources (Grants No. 200701039 and 200801001) and the National Technology Supporting Program (Grants No. 2006BAC05B02 and 2007BAC03A060301).
*Corresponding author (e-mail: *yanxiakang@126.com*)
Received May 30, 2009; accepted Sep. 11, 2009

recommended that soil evaporation be simulated based on the equations of heat flow at the soil surface, which includes vapor diffusion and a semi-empirical correction function for the surface vapor pressure. Wallace et al. (1999) found that the Ritchie (1972) approach was unable to predict daily soil evaporation accurately, but can provide good estimates of cumulative soil evaporation over hydrologically significant periods. Aydin et al. (2005) provided an empirical formula on the basis of potential and actual soil evaporation and soil-water potential in the surface layer of the soil, which has been successfully applied in semiarid areas. Bittelli et al. (2008) implemented a fully coupled numerical model to solve the governing equations for liquid water, water vapor, and heat transport in bare soils.

The second problem is how to determine soil evaporation not only from a uniform surface but also from a heterogeneous surface, as well as the way in which soil evaporation is spatially distributed. Soil evaporation calculated in traditional ways can only represent the evaporation around meteorological stations, so evaporation in other areas with no meteorological data or an insufficient amount of data is hard to determine. With remote sensing data, it is possible to solve this problem. First, some detailed information about the heterogeneous land surface can be obtained from remote sensing data because of its high spatial resolution and abundance of information. Second, combining land surface parameters with evaporation models can illuminate spatial distribution patterns of soil evaporation. Moran et al. (1996) combined the Penman-Monteith model with temperature and reflectivity acquired from remote sensing data to study the soil evaporation of a region with partial canopy cover. Chanzy et al. (1995) combined microwave and infrared data to estimate soil evaporation with a semi-empirical correction function. Qiu et al. (1998, 2006) proposed a model based on three different temperatures to simulate the spatial distribution of soil evaporation.

There are many models for estimating soil evaporation, but it is unknown which methods are the most accurate and useful. It is vital to compare and analyze the performance of different models to provide a reference for further study. Based on ASTER (Advanced Spaceborne Thermal Emission and Reflection Radiometer) remote sensing data, this study compared and analyzed the evaporation estimated by three models (the Penman-Monteith model, the Priestey-Talyor model, and the aerodynamics model), and investigated the error of the three models to determine which one is most suitable for the Heihe River Basin.

2 Description of models

2.1 Flow for evaporation estimation

Two major categories of models used to estimate soil evaporation are remote sensing models and micrometeorological models. Remote sensing models are based on the energy balance principle and evaporation is obtained as the residual of the energy budget theorem. In the energy balance equation, sensible heat flux is critical and influenced by many factors,

which makes it difficult to obtain. Much research has been devoted to this problem, but a solution has not yet been developed. Micrometeorological models that have frequently been used for estimating evaporation include the Penman-Monteith model (P-M model) (Aydin et al. 2005), the Priestey-Talyor model (P-T model) (Desborough et al. 1996), and the aerodynamics model (P-K model). When estimating evaporation with the P-M model and P-T model, net radiation is a vital parameter. However, stations that measure net radiation are scarce; there are not enough of them to apply in the model. When estimating evaporation with the P-K model, the saturated vapor pressure of the soil surface is difficult to obtain. All the disadvantages described above have impeded the application of these models. The problems can be solved by combining remote sensing data with micrometeorological models: if the variables that are difficult to obtain in traditional ways can be obtained from remote sensing data, micrometeorological models can effectively estimate evaporation. This study made use of the P-M model, P-T model, and P-K model to estimate evaporation in the Heihe River Basin. After comparison and analysis, a suitable evaporation model for the Heihe River Basin was chosen. Fig. 1 describes the model structure.

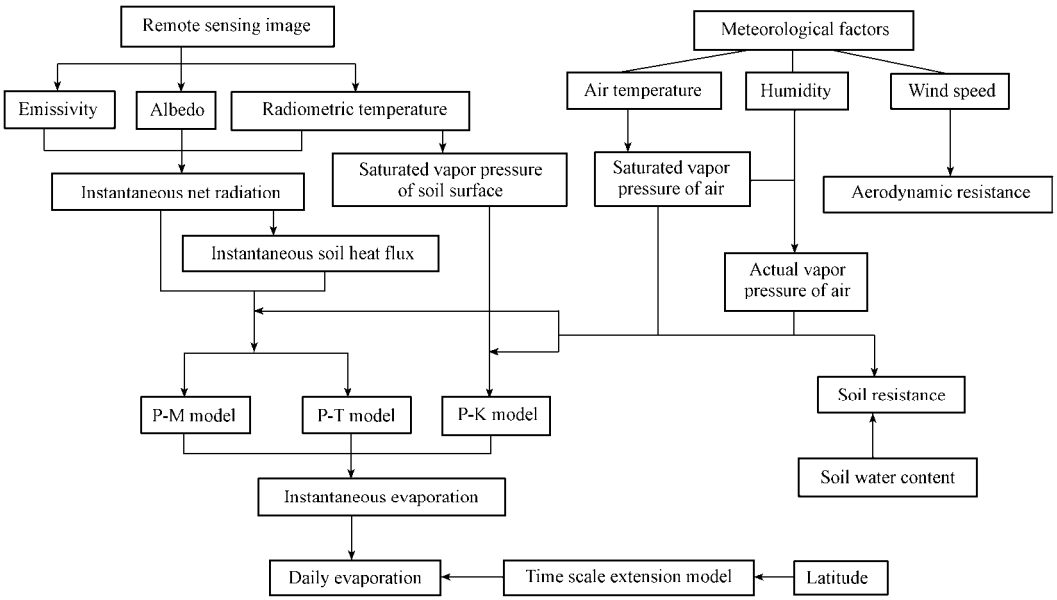

Fig. 1 Flow chart for evaporation estimation

2.2 Estimation of model parameters

Net radiation is a vital parameter for estimating evaporation with the P-M and P-T models. However, in the Heihe River Basin, whose area is 1.429×10^5 km^2, there are only three stations that measure radiation. They do not provide data with a sufficiently wide spatial distribution for estimating evaporation from a basin whose terrain and underlying soil and

geology are complex. The net radiation can be obtained from remote sensing data. Because remote sensing data is instantaneous, the net radiation is also instantaneous at the corresponding time (Liu et al. 2004):

$$R_{\mathrm{n}} = (1-\alpha)R_{\mathrm{s(in)}} + \varepsilon_{\mathrm{s}}R_{\mathrm{L(in)}} - R_{\mathrm{L(out)}} = (1-\alpha)R_{\mathrm{s(in)}} + \varepsilon_{\mathrm{s}}\varepsilon_{\mathrm{a}}\sigma T_{\mathrm{a}}^4 - \varepsilon_{\mathrm{s}}\sigma T_{\mathrm{s}}^4 \tag{1}$$

$$\varepsilon_{\mathrm{a}} = 1.24(e_{\mathrm{a}}/T_{\mathrm{a}})^{1/7} \tag{2}$$

where R_{n} is the net radiation (MJ/(m^2·h)); α is the reflectivity of the soil surface; $R_{\mathrm{s(in)}}$ is the downward short-wave radiation (MJ/(m^2·h)); $R_{\mathrm{L(in)}}$ is the downward long-wave radiation (MJ/(m^2·h)); $R_{\mathrm{L(out)}}$ is the upward long-wave radiation (MJ/(m^2·h)); ε_{s} is the emissivity of the soil surface; ε_{a} is the emissivity of air; T_{a} and T_{s} are temperatures at the atmospheric level and land surface (K), respectively; σ is the Stefan-Boltzmann constant; and e_{a} is the actual vapor pressure (kPa).

Reflectivity can be written as (Liang 2001)

$$\alpha = 0.484\alpha_1 + 0.335\alpha_3 - 0.324\alpha_5 + 0.551\alpha_6 + 0.305\alpha_8 - 0.367\alpha_9 - 0.0015 \tag{3}$$

where α_1, α_3 α_5, α_6, α_8, and α_9 represent the albedos of bands 1, 3, 5, 6, 8, and 9, respectively.

Soil heat flux G (MJ/(m^2·h)) can be estimated from the net radiation and land surface temperature values according to Zhang et al. (2005):

$$G = 0.084R_{\mathrm{n}} + 1.8(T_{\mathrm{s}} - 273.16) \tag{4}$$

The variable r_{a} (s/m) is the aerodynamic resistance, which can be defined as

$$r_{\mathrm{a}} = \left[\ln\left(\frac{z-d}{z_{0\mathrm{m}}}\right) - \psi_{\mathrm{sm}}\right]\left[\ln\left(\frac{z-d}{z_{0\mathrm{h}}}\right) - \psi_{\mathrm{sh}}\right] \Big/ (k^2 u) \tag{5}$$

where z is the measured height (m); d is the zero-plane displacement height (m); $z_{0\mathrm{m}}$ and $z_{0\mathrm{h}}$ are the roughness length governing momentum and vapor transfer (m), respectively; ψ_{sm} is the stability correction for buoyancy effects on the momentum flux; ψ_{sh} is the stability correction for heat transport; k is the von Karman's constant (k = 0.41); and u is the wind speed at the measured height (m/s). The soil types in the Heihe River Basin are complicated and various. According to Liu and Dong (2003), the mean $z_{0\mathrm{m}}$ of sandy soil is 0.01. Estimates of $z_{0\mathrm{h}}$, ψ_{sm}, and ψ_{sh} can be obtained from Li and Zhao (2006).

Soil resistance is affected by soil type and soil water content and can be obtained from an empirical formula (Sun et al. 1998):

$$r_{\mathrm{s}} = \exp(8.2 - 4.225\theta/\theta_{\mathrm{s}}) \tag{6}$$

where r_{s} is the soil resistance (s/m), θ is the soil water content, and θ_{s} is the saturated soil

water content.

The saturated vapor pressure of the soil surface e_b is important to the P-K model, and can be estimated from the land surface temperature T_s. The land surface temperature is an instantaneous value, so the saturated vapor pressure of the soil surface is also instantaneous. The model is as follows:

$$e_b = 0.611\exp\left(\frac{17.27T_s}{T_s + 237.3}\right) \tag{7}$$

2.3 Description of models

The P-M model (Aydin et al. 2005), the P-T model, and the P-K model (Desborough et al. 1996; Meng and Cui 2007) are as follows:

$$E_{PM} = \frac{1}{\lambda}\frac{\Delta(R_n - G) + 3.6\rho C_p(e_s - e_a)/r_a}{\Delta + \gamma(1 + r_s/r_a)} = E_{Rn} + E_{aero} \tag{8}$$

$$E_{PT} = 1.72\frac{1}{\lambda}\frac{\Delta(R_n - G)}{\Delta + \gamma(1 + r_s/r_a)} \tag{9}$$

$$E_{PK} = \frac{1}{\lambda}\frac{3.6\rho C_p(e_b - e_a)}{\gamma r_a}\beta = \frac{1}{\lambda}\frac{3.6\rho C_p(e_b - e_a)/r_a}{\gamma(1 + r_s/r_a)} \tag{10}$$

$$\beta = \frac{1}{(1 + r_s/r_a)} \tag{11}$$

where E_{PM} is the hourly soil evaporation estimated by the P-M model (mm/h); ρ is the air density (kg/m^3); C_p is the specific heat of air (C_p = 1.013 kJ/(kg·℃)); e_s is the saturated vapor pressure (kPa); Δ is the slope of the saturated vapor pressure-temperature curve (kPa/℃); γ is the psychometric constant (kPa/℃); λ is the latent heat of vaporization (MJ/kg); 3.6 is the factor for conversion from kJ/s to MJ/h; E_{Rn} is the evaporation caused by radiation (mm/h); E_{aero} is the evaporation caused by aerodynamics (mm/h); E_{PT} is the hourly soil evaporation estimated by the P-T model (mm/h); E_{PK} is the hourly soil evaporation estimated by the P-K model (mm/h); and β is the effective wet parameter (Alvenäs and Jansson 1997). The values of Δ, γ, λ, e_s, and e_a can be estimated from meteorological data.

2.4 Daily evaporation

Because the remote sensing data is instantaneous, the meteorological data is instantaneous as well, and consistent in time with the remote sensing data. The soil evaporation estimated from remote sensing data is also instantaneous, but we need daily soil evaporation data to run the models. Daily soil evaporation data should be obtained. This study

used the sine relationship principle (Xie 1991) to generate daily evaporation data from instantaneous evaporation data:

$$E_{\mathrm{d}} = E\frac{2N_{\mathrm{E}}\sin\left(\pi t/N_{\mathrm{E}}\right)}{\pi} \tag{12}$$

$$N_{\mathrm{E}} = a + b\sin\left[2\pi\left(D+10\right)/365\right] \tag{13}$$

$$a = 12.0 - 5.69\times10^{-2}\phi - 2.02\times10^{-4}\phi^2 + 8.25\times10^{-6}\phi^3 \tag{14}$$

$$b = 0.123\phi - 3.10\times10^{-4}\phi^2 + 8.00\times10^{-7}\phi^3 + 4.99\times10^{-7}\phi^4 \tag{15}$$

where E_{d} is the daily evaporation (mm/d); E is the instantaneous evaporation, which can be obtained from the P-M model, the P-T model, or the P-K model (mm/h); t is the time the satellite passed; N_{E} is the number of hours of daily evaporation; D is the ordinal number of the corresponding days in a year; a and b are coefficients defined in Eqs. (14) and (15); and ϕ is the latitude.

3 Study area and materials

3.1 Description of study area

The Heihe River Basin is the second-largest inland river basin in northwestern China. It ranges from longitudes of 97°20′E to 102°12′E and latitudes of 37°50′N to 42°40′N. Yingluoxia is the boundary between the upper reaches and middle reaches, and Zhengyixia is the boundary between the middle reaches and lower reaches. The average annual temperature is 2℃ and the average annual precipitation is 350 mm in the upper basin. Along the middle reaches of the basin, the average annual temperature is between 6℃ and 8℃, the average annual precipitation is 140 mm, and the average annual potential water evaporation is 1410 mm. In the lower basin, an extremely arid area, the average annual temperature is between 8℃ and 10℃, the average annual precipitation is 47 mm, and the average annual potential water evaporation is 2250 mm.

3.2 Meteorological data

There are 21 weather stations around the study area. The locations of these stations are shown in Fig. 2. Hourly data of the mean temperature, maximum temperature, minimum temperature, wind speed, vapor pressure, and atmospheric pressure for the years 2000 through 2003 were selected and interpolated to a grid of 1.5-km cells using the inverse distance method. At the same time, soil water content data from seven stations were selected and interpolated to a grid of 1.5-km cells in the same way. Daily water evaporation at weather stations and at Dayekou Station along with actual evaporation at Dayekou Station for the years 2004 through

2006 were selected as well.

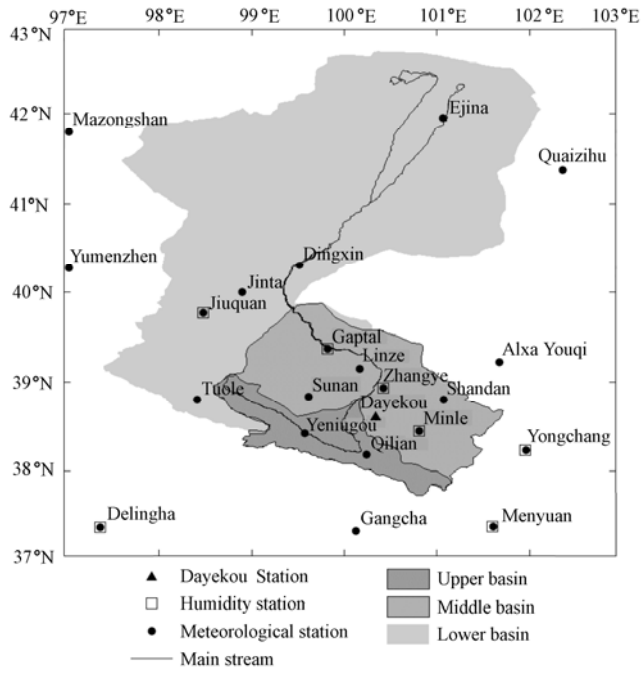

Fig. 2 Heihe River Basin

3.3 Remote sensing data

ASTER is a sensor on the Terra satellite, which was launched by the U.S. in 1999. ASTER is a multi-spectrum sensor with a high spatial resolution. It has a visible wave band spectrum and an infrared wave band spectrum. Compared with other satellites, the advantages of ASTER are that the data is free, the spatial resolution is high, and the information from wave bands is more abundant. It has 14 wave bands and three subsystems (Li and Tian 2004), which contain three visible and near infrared reflector (VNIR) wave bands with a 15-m spatial resolution, six shortwave infrared reflector (SWIR) wave bands, and five thermal infrared reflector (TIR) wave bands. This study collected 15 remote sensing images in which the land is only bare soil to determine the most suitable model, and 12 remote sensing images to analyze the spatial distribution. The scope is different in different images.

3.4 Pre-processing of remote sensing data

The data format is ASTER L1b, which has been processed only through radiation correction and coarse geometric correction. In order for this data to be used, it should be pre-processed. The procedure is to apply radiometric calibration atmosphere correction, transformation of the projection, fine geometric correction, and enhancing of the remote sensing information.

4 Results and analysis

4.1 Daily soil evaporation comparison

The daily evaporation estimated by the three models is shown in Fig. 3. The cumulative ASTER image is from the years 2000 through 2003, and the cumulative actual evaporation at Dayekou Station is from the years 2004 through 2006. To obtain the actual evaporation at Dayekou Station for the years 2000 through 2003, we analyzed the water evaporation and actual evaporation of the years 2004 through 2006. Results indicated a proportional relationship between water evaporation and actual evaporation, providing for a monthly correction coefficient. We then obtained actual evaporation for the years 2000 through 2003 by multiplying the monthly correction coefficient by water evaporation for those years. As shown in Fig. 3, E_{PM} is greater than actual evaporation for the months of October and November, and lesser for other months. E_{PT} is less than the actual evaporation for the months of March, April, and November, and greater for other months. E_{PK} is greater than the actual evaporation for the months of March, April, and November, and lesser for other months.

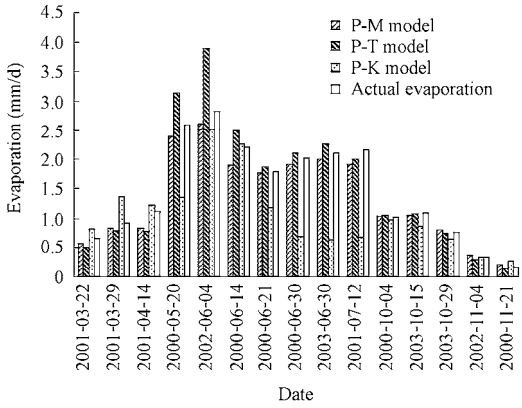

Fig. 3 Comparison of calculated evaporation with actual evaporation

Table 1 shows that the mean of the absolute value of relative error is 9% for the P-M model, 14% for the P-T model, and 32% for the P-K model.

Table 1 Relative errors of E_{PM}, E_{PT}, and E_{PK}

Date	Relative error (%)			Date	Relative error (%)		
	E_{PM}	E_{PT}	E_{PK}		E_{PM}	E_{PT}	E_{PK}
2001-03-22	−13	−24	22	2003-06-30	−4	7	−70
2001-03-29	−9	−14	48	2001-07-12	−11	−8	−68
2001-04-14	−25	−30	9	2000-10-04	2	3	−3
2000-05-20	−7	21	−47	2003-10-15	−2	−1	−20
2002-06-04	−7	38	−10	2003-10-29	6	−1	−14
2000-06-14	−13	13	3	2002-11-04	8	−11	0
2000-06-21	−1	4	−34	2000-11-21	16	−22	55

2000-06-30	−5	4	−66

4.2 Sources of error

According to this analysis, the P-M model has the smallest amount of error and the P-K model has the largest. All three models are micrometeorological models and have some common features. The P-M model is based on the energy balance and aerodynamics, and E_{Rn} and E_{aero} were estimated independently. The P-T model is only based on the energy balance and is simplified from the P-M model, treating E_{aero} as 0.72 times the value of E_{Rn}. The P-K model is based only on the aerodynamics. According to Eqs. (8) and (10), the main difference between the P-M model and the P-K model is in the vapor pressure difference. The vapor pressure difference of the P-M model is the difference between e_{s} and e_{a}, and the vapor pressure difference of the P-K model is the difference between e_{b} and e_{a}. As shown in Table 2, for the months of November through April of next year the net radiation and precipitation are small, so the evaporation mainly comes from the contribution of E_{aero}. Because e_{b} is greater than e_{s}, E_{PK} is larger than E_{PM}. For other months, the evaporation mainly comes from the contribution of E_{Rn}, so E_{PK} is smaller than E_{PM}. The derivation of the P-M model assumes a uniform underlying surface and non-advection conditions, so the error source of the P-M model is the neglect of the estimation of advection.

Table 2 Mean meteorological values in different months in 2000-2003

Month	P_{r}* (mm)	R_{n} (MJ/(m^2·d))	u (m/s)	T_{a} (℃)	T_{s} (℃)	Month	P_{r} (mm)	R_{n} (MJ/(m^2·d))	u (m/s)	T_{a} (℃)	T_{s} (℃)
Jan.	3.0	3.4	1.7	−8.6	−2.4	Jul.	24.7	10.2	2.2	23.3	36.3
Feb.	1.2	4.5	2.0	−4.1	3.8	Aug.	25.5	9.3	2.1	21.1	34.0
Mar.	2.0	5.7	2.3	3.1	13.2	Sep.	24.3	8.4	1.8	15.5	27.7
Apr.	4.1	6.6	2.6	10.7	20.7	Oct.	4.9	7.2	1.6	7.5	19.6
May	15.0	9.7	2.3	16.5	28.6	Nov.	2.4	3.5	1.7	−0.3	8.6
Jun.	18.8	10.4	2.2	21.1	32.9	Dec.	1.9	2.9	1.7	−7.9	−2.3

Note: P_{r} is precipitation.

The parameters of the P-M model, the P-T model and the P-K model are different. In some areas, because of insufficient data for estimating evaporation with the P-M model, the results of the P-T model and the P-K model can provide a reference. There are eight (or seven) parameters in the P-M model: T_{a} (mean air temperature), P (atmospheric pressure), θ, θ_{s}, u, e_{a} (or relative humidity H_{R}), G (or T_{s}, or $0.2R_{\mathrm{n}}$), and R_{n}. There are seven (or six) parameters in the P-T model: T_{a}, P, θ, θ_{s}, u, G (or T_{s}, or $0.2R_{\mathrm{n}}$), and R_{n}. There are seven parameters in the P-K model: T_{a}, P, θ, θ_{s}, u, T_{s}, e_{a} (or H_{R}). Unlike the P-M model, the P-T model does not need data for e_{a} (or H_{R}), and the P-K model does not need data for R_{n}. When there is a lack of e_{a} data, the P-T model can be

used to estimate evaporation, and when there is a lack of R_n data, the P-K model can be used to estimate evaporation.

4.3 Analysis of spatial distribution

The P-M model is the most suitable of these three models, so the results of the P-M model were used to analyze the spatial distribution of evaporation in the Heihe River Basin. The mapping band of ASTER is 60 km × 60 km, so the ASTER image of a certain day can only cover part of the Heihe River Basin. The spatial distribution can only be analyzed at different times and scopes. Seven images from October 29, 2003 and five images from November 15, 2001 were selected to mosaic and analyze the spatial distribution of evaporation. The images from October 29, 2003 (Fig. 4) are of the eastern part of the Heihe River Basin, which is covered mostly by soil and partly by desert, with a spot of vegetation and water. The area of vegetation and water was neglected in analyses. The elevation increased from 1000 m in the north to 3000 m in the south, and the precipitation from October 10 to October 29 was only 9.6 mm. The soil water content was only 51%. The evaporation from the desert area was between 1.0 mm/d and 2.0 mm/d, the soil evaporation was less than 0.5 mm/d in the northern district, and the evaporation was between 0.5 mm/d and 1.0 mm/d in the southern district because of the strong water-holding capacity of vegetation. The image from November 15, 2001 (Fig. 5) is of the western part of the Heihe River Basin. The elevation is between 1 000 m and 1300 m, and the mean temperature on that day was around 4℃. The precipitation from October 1 to November 15, 2001 was only 2.9 mm. The soil water content was low, so the evaporation was less than 0.4 mm/d. Evaporation from the southern district was less than 0.2 mm/d, evaporation from the western district was between 0.3 mm/d and 0.4 mm/d, and evaporation from other districts was between 0.2 mm/d and 0.3 mm/d.

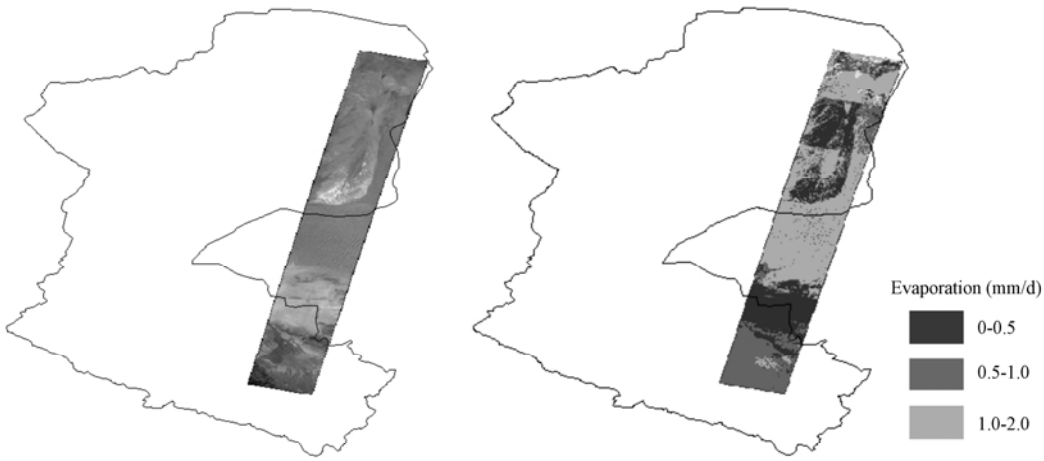

(a) ASTER image (b) Evaporation

Fig. 4 ASTER image and spatial distribution of evaporation on October 29, 2003

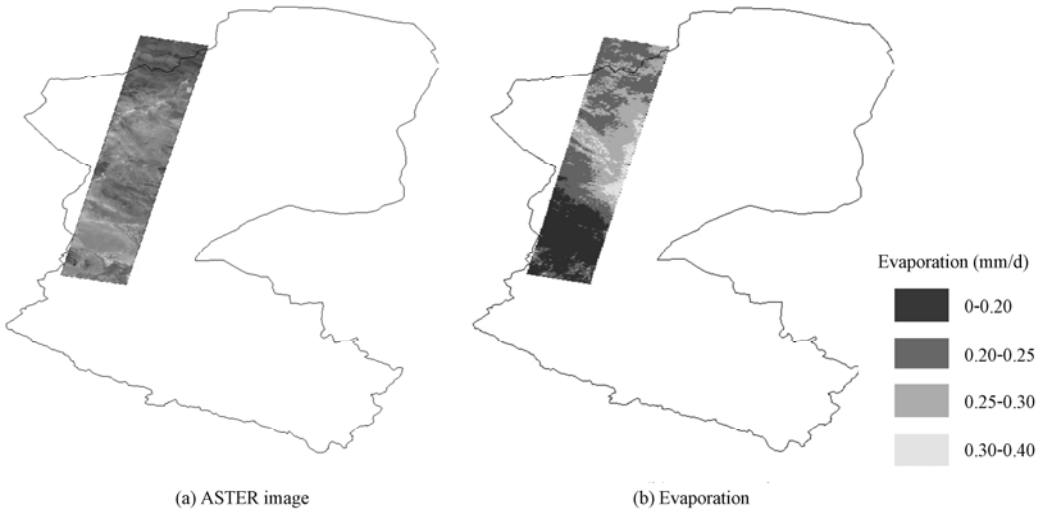

Fig. 5 ASTER image and spatial distribution of evaporation on November 15, 2001

5 Conclusions

This study estimated bare soil evaporation based on ASTER remote sensing data combined with the P-M model, P-T model, and P-K model, respectively. The evaporation simulated by each of the three models was compared with actual evaporation. Sources of error have been discussed. The main conclusions are as follows:

(1) The mean absolute relative error was 9% for the P-M model, 14% for the P-T model, and 32% for the P-K model. The P-M model is the best of these three models for estimating the bare soil evaporation.

(2) The error source of the P-M model is the neglect of advection estimation. The error source of the P-T model is the simplification of the component of aerodynamics as 0.72 times the net radiation. The error source of the P-K model is in the difference of vapor pressure.

(3) The spatial distribution of bare soil evaporation is evident, and the evaporation is mainly influenced by soil water content, elevation, and meteorological data.

References

Alvenäs, G., and Jansson, P. E. 1997. Model for evaporation, moisture and temperature of bare soil: Calibration and sensitivity analysis. *Agricultural and Forest Meteorology*, 88(1-4), 47-56. [doi:10.1016/S0168-1923(97)00052-X]

Aydin, M., Yang, S. L., Kurt, N. and Yano, T. 2005. Test of a simple model for estimating evaporation from bare soils in different environments. *Ecological Modelling*, 182(1), 91-105. [doi:10.1016/j.ecolmodel.2004.07.013]

Bittelli, M., Ventura, F., Campbell, G. S., Snyder, R. L., Gallegati, F., and Pisa, P. R. 2008. Coupling of heat, water vapor, and liquid water fluxes to compute evaporation in bare soils. *Journal of Hydrology*, 362(3-4), 191-205. [doi:10.1016/j.jhydrol.2008.08.014]

Chanzy, A., Bruckler, L., and Perrier, A. 1995. Soil evaporation monitoring: A possible synergism of microwave and infrared remote sensing. *Journal of Hydrology*, 165(1-4), 235-259. [doi:10.1016/0022-1694(94)02571-R]

Desborough, C. E., Pitman, A. J., and Irannejda, P. 1996. Analysis of the relationship between bare soil evaporation and soil moisture simulated by 13 land surface schemes for a simple non-vegetated site. *Global and Planetary Change*, 13(1), 47-56. [doi:10.1016/0921-8181(95)00036-4]

Li, H. T., and Tian, Q. J. 2004. An introduction to ASTER data and ASTER mission. *Remote Sensing Information*, (3), 53-55. (in Chinese)

Li, S. B., and Zhao, C. Y. 2006. Estimating evapotranspiration based on energy balance in Guanchuan River Basin using remote sensing. *Remote Sensing Technology and Application*, 21(6), 521-526. (in Chinese)

Liang, S. L. 2001. Narrowband to broadband conversions of land surface albedo. *Remote Sensing of Environment*, 76(2), 213-238. [doi:10.1016/S0034-4257(00)00205-4]

Liu, X. P., and Dong, Z. B. 2003. Review of aerodynamic roughness length. *Journal of Desert Research*, 23(4), 337-346. (in Chinese)

Liu, Z. W., Lei, Z. D., Dang, A. R., and Yang, S. X. 2004. Remote sensing and the SEBAL model for estimating evapotranspiration in arid regions. *Journal of Tsinghua University (Science and Technology)*, 44(3), 421-424. (in Chinese)

Meng, C. L., and Cui, J. Y. 2007. Study on soil evaporation and coupling transmission of soil moisture and heat in arid areas. *Arid Zone Research*, 24(2), 141-145. (in Chinese)

Moran, M. S., Rahman, A. F., Washburne, J. C., Goodrich, D. C., Weltz, M. A., and Kustas, P. 1996. Combining the Penman-Monteith equation with measurements of surface temperature and reflectance to estimate evaporation rates of semiarid grassland. *Agricultural and Forest Meteorology*, 80(2-4), 87-109. [doi:10.1016/0168-1923(95)02292-9]

Qiu, G. Y., Yano, T., and Momii, K. 1998. An improved methodology to measure evaporation from bare soil based on comparison of surface temperature with a dry soil surface. *Journal of Hydrology*, 210(1-4), 93-105. [doi:10.1016/S0022-1694(98)00174-7]

Qiu, G. Y., Shi, P. J., and Wang, L. M. 2006. Theoretical analysis of a remotely measurable soil evaporation transfer coefficient. *Remote Sensing of Environment*, 101(3), 390-398. [doi:10.1016/j.rse.2006.01.007]

Ritchie, J. T. 1972. Model for predicting evaporation from a row crop with incomplete cover. *Water Resources*, 8(5), 1204-1213.

Sun, S. F., Niu, G. Y., and Hong, Z. X. 1998. A water and heat transport model in arid and semiarid regions. *Scientia Atmospherica Sinica*, 22(1), 1-10. (in Chinese)

Wallace, J. S., Jackson, N. A., and Ong, C. K. 1999. Modelling soil evaporation in an agroforestry system in Kenya. *Agricultural and Forest Meteorology*, 94(3-4), 189-202. [doi:10.1016/S0168-1923(99)00009-X]

Xie, X. Q. 1991. Estimation of daily evapo-transpiration (ET) from one time-of-day remotely sensed canopy temperature. *Journal of Remote Sensing*, 6(4), 253-260. (in Chinese)

Zhang, C. C., Wang, G. Q., Wei, J. H., and Shao, J. L. 2005. Estimates of evapotranspiration based on TM and NOAA data in the Yellow River Delta. *Journal of Tsinghua University (Science and Technology)*, 45(9), 1184-1188. (in Chinese)